# Electric-Field Dependence of Linear Optical Properties in Quantum Well Structures: Waveguide Electroabsorption and Sum Rules

DAVID A. B. MILLER, JOSEPH S. WEINER, AND D. S. CHEMLA
(*Invited Paper*)

*Abstract*—**We summarize the electric-field dependence of absorption and luminescence in quantum wells for fields perpendicular to the layers, present extended discussion of electroabsorption spectra and devices in waveguide samples, and derive sum rules for electroabsorption. Optical bistability, self-linearized modulation, and optical level shifting are demonstrated in self-electrooptic effect device configurations, with good modulation contrast and polarization-dependent properties. The electroabsorption spectra enable quantitative comparison of theory and experiment for absorption strengths in quantum wells with field. The sum rules enable excitonic effects to be included in the comparison, and good agreement is seen. One sum rule is also more generally applicable to electroabsorption in semiconductors.**

## I. Introduction

In recent years, the optical properties of quantum wells (QW's) have been the subject of increasing interest. The linear optical behavior has long been known to show much interesting structure that reflects the quantum confinement of the carriers [1]. Some more recent studies have concentrated on the nonlinear optical properties [2] and the electric-field dependence of the linear properties (e.g., electroabsorption) [3]–[37], particularly those associated with the exciton absorption resonances near the bandgap energy. Both of these have proved to be fruitful areas of study, and it is some aspects of the second that will concern us here.

One reason for increased interest in both of these areas is the possibility of practical applications. Exciton resonances in bulk material have interesting nonlinear absorption and electroabsorption properties, but these are largely restricted to low temperatures. In QW's, however, the exciton resonances are clearly resolvable at room temperature (see [2] for a discussion of room-temperature QW excitons). As a result, these resonances can be exploited in QW's. The QW room-temperature excitonic absorption saturates in a manner superficially similar to that of low-temperature bulk materials, although there are important differences in the detailed mechanisms, such as the relative importance in Coulomb screening [38]. One application of this nonlinearity is to passive mode locking of laser diodes with stable trains of single pulses [39]. For electroabsorption with fields parallel to the QW layers [20], the effects are also similar to those of bulk semiconductors, except that they can be seen very clearly at room temperature; one possible application of this is to subpicosecond electrooptic samplers for measurements of very fast electrical transients [36]. However, perhaps the largest variety of speculative devices using room-temperature QW optical properties relies on the consequences of electric fields perpendicular to the QW layers [4], [8], [9], [12], [14], [15], [16], [19], [22], [24], [25], [26], [28]–[30], [33]. Two effects are seen in this configuration that are of device interest. In luminescence, the light emission can be quenched with field, suggesting applications to modulation of light sources [4], [15], [16]. In absorption, the band edge can be shifted to lower photon energies with applied fields, while still retaining the excitonic resonances. This electroabsorptive effect has been called the quantum-confined Stark effect (QCSE) [10], [20]. The QCSE is obviously qualitatively different from bulk electroabsorption at any temperature. It is therefore particularly interesting both from a practical and a fundamental viewpoint, and it forms the basis for a variety of modulators [8], [12], [14], [22], [24], [26], [28]–[30], [33] and optical switching devices [9], [19].

In this paper, in addition to a brief summary of electric-field effects on QW optical properties, we will be concerned with the QCSE in QW waveguides, presenting an extended discussion of experimental results [29] and some devices in waveguides containing only two QW's. The waveguide enables both distinct optical polarizations to be investigated, showing clear selection rules. It also gives particularly clear spectra because there is no field inhomogeneity as in multiple QW measurements, while still allowing absolute measurements of absorption strength not complicated by quantum efficiencies of photodetection or luminescence. We are able to examine the broadening of exciton resonances with field, and we can use the absolute

Manuscript received March 6, 1986.
The authors are with AT&T Bell Laboratories, Holmdel, NJ 07733.
IEEE Log Number 8609345.

absorption measurements to compare absorption strengths in the presence of perpendicular fields to theory.

To compare theory and experiments for absorption strengths, we will also derive sum rules for electroabsorption. One of the rules that we derive is applicable to electroabsorption in general, and the other two give more specific information for quantum wells.

This paper is organized as follows. In Section II, we briefly summarize some related work. In Section III, we present our experimental results in the QW waveguide. We show results for a variety of device configurations. We present the detailed spectra for electroabsorption in both polarizations and analyze these in the light of extended calculations of shifts and overlap integrals. To attempt to explain some empirical observations, sum rules for electroabsorption are derived in Section IV and are compared to experiment. Finally, we draw our conclusions in Section V.

## II. Summary of Electric-Field Dependence of Quantum Well Optical Properties

The history of this subject is brief, but active. We have listed some of the work most directly relevant in approximate chronological order in [3]–[38]. The first interest in electric-field dependence of quantum well optical properties was in their luminescence behavior [3], [4]. For fields perpendicular to the quantum well layers, the luminescence was observed to quench in relatively narrow wells ($\sim 30$ Å) [3] with moderately large fields on the order of $10^4$ V/cm. Independently, a device was proposed that would rely on just such a property [4]. In absorption, large changes in absorption were observed in somewhat larger wells ($\sim 100$ Å) [6], [8]. In particular, it was concluded [8] that perpendicular fields resulted in large shifts in absorption, including the exciton resonances, to lower photon energies in a manner quite unlike the electroabsorption in bulk semiconductors. The electroabsorption was of obvious applicability to optical modulators [8], and another class of nonlinear optical devices relying on this electroabsorption [the self-electrooptic effect device (SEED)] followed [9].

The first quantitative attempt at explaining the luminescence behavior was in terms of reduced overlap of electron and hole wave functions [5]. This was not successful as an explanation for the initial measurements [3], although it was important for the subsequent explanation of the electroabsorption phenomena. Subsequent time-resolved luminescence measurements [17] showed a decrease of luminescence lifetime with field in these samples, qualitatively consistent with tunneling of carriers out of the well as being the dominant lifetime. The electroabsorption was successfully explained through a mechanism called the quantum-confined Stark effect (QCSE) [10], [20]; independently, many parts of this mechanism were also proposed [11] as an extension of the work of [5]. Recently, it was observed that luminescence lifetime could be increased with field in samples with well widths more comparable to those used in absorption [31], in approximate quantitative agreement with the overlap mechanism [5] and in a manner consistent with the QCSE. Here we will outline the key features of both luminescence and absorption behavior and their explanations from the viewpoint of the QCSE.

In absorption or luminescence, we are concerned with an electron–hole pair, either in creation or destruction. The photon energy at which we see absorption or emission will be approximately the pair state energy calculated in the absence of a radiation field. This is the approach that has been taken in all of the theory so far. The strength of the transitions is not usually strong enough to warrant a dressed state approach. In general, the electron and hole interact with each other through the Coulomb interaction, and this excitonic effect should ideally be included in evaluating the states of the system [10], [11], [20], although most theoretical papers choose to neglect it [5], [18], [21], [23], [27]. The confinement of the particles is usually in such a large volume that an effective mass envelope function approach can be used, although some possible effects of going beyond this approximation have been noted [23]. In the presence of the field, there are, strictly speaking, no bound states of the system, but it is presumed that those states of interest live long enough to give a well-defined optical transition; in some theoretical work, this width is calculated [10], [21], [20], [23], [40]. The strength of the transition in the envelope function approximation is usually presumed proportional to the probability of finding the electron and hole in the same unit cell (we will discuss the validity of this below); if excitonic effects are neglected, this reduces to the square of the electron–hole overlap integral in the direction perpendicular to the layers. The theories therefore calculate the energy levels of the pair states, the widths of the "states" in energy, and the absorption probabilities.

Because of the effective mass envelope function approximation, the problem of the electron–hole pair states reduces to the analysis of generalized hydrogen atom states in an electric field. The masses and dielectric constant are different and nonisotropic, but the principal qualitative difference compared to the Stark shifts in a hydrogen atom is the addition of a confining potential. Hence, we can define this problem as a quantum-confined Stark effect [10], [20]. As with other excitonic problems, the energies of the pair states will be the bandgap energy plus the hydrogenic energy. This remains true in the presence of field.

In this QCSE approach [10], [20], the Hamiltonian of the electron and hole includes confinement potentials, electrostatic potentials, and electron–hole interaction. This has been solved by a variety of approximation methods [10], [11], [20] for the lowest states, corresponding to the lowest excitonic resonances. The absorption behavior for fields perpendicular to the layers shows large shifts of the exciton peaks to lower energies, with the peaks remaining resolved, although losing some area. The QCSE approach can explain all of these phenomena. As the field is applied, the electron and hole are pulled to opposite

sides of the well. Consequently, the potential energy of the pair is reduced because the charges have moved towards the electrodes, generating a polarization. Partly compensating for this reduction is the increase in kinetic energies of the particles as they are confined more tightly near the walls of the well and the reduction in the Coulomb attraction of the electron and hole. Calculations of the energies of the exciton peaks including these effects agree well with experiments [10], [11], [20]. The dominant terms in the energy shifts are the "single-particle" kinetic and potential energies. The electron–hole Coulomb interaction tends to saturate out as the particles are pulled to the opposite sides of the well, and the effect of this term is only just significant in comparing theory and experiment for the energies [10], [20]. The existence of significant electron–hole interaction even at high fields is, however, very important. It is the Coulomb interaction that correlates the motion of electron and hole, especially in the plane of the layers, increasing the probability of finding the electron and hole in the same unit cell, and hence creating a strong absorption feature. If there were not a strong interaction, then there would be no exciton resonance at high fields.

Two further calculations are necessary to complete the picture in absorption. First, we must be sure that the exciton state once deformed by the field is long enough lived to present a sharp resonance. This was checked in the original QCSE calculations [10], [20] by evaluating the quasi-bound energy levels of the single-particle states using a tunneling resonance technique. The center of the resonance in transmission gives the energy level position and the width gives the (inverse) lifetime; these widths were found to be sufficiently low, so that tunneling (i.e., field emission) of individual electrons and holes out of the wells would not destroy the absorption resonances for the samples used in these experiments. Other calculational methods are available for the effective width of the states [21], [23], [40]. The second calculation relates to the strength of the transitions. Qualitatively, there is no problem here, in that the probability of finding the electron and hole in the same unit cell should certainly decrease as the field is applied, and consequently, the absorption probability should decrease, in agreement with experiment. To date, however, this has not been completely calculated. All that is usually evaluated is the overlap of electron and hole wavefunctions in the direction perpendicular to the layers; in the limit that the wavefunction in the plane of the layers is not changed by the applied field, this would be a correct approach. This is not valid for exciton resonances since the wavefunction in the plane is determined by the electron–hole Coulomb interaction which is strongly perturbed by the electric field perpendicular to the layers as discussed above; to be specific, the exciton orbit becomes larger in the plane with increasing field perpendicular to the plane. No successful quantitative comparison between theory and experiment has so far been presented for the case of absorption strength. We will consider this point later in this paper, and we will show that by the consideration not of a single transition, but of whole sets of transitions, satisfactory agreement can be obtained through the use of sum rules.

The persistence of the exciton resonances at high fields strongly contrasts with the behavior in bulk material and in QW's for fields parallel to the layers [20] where the absorption resonances disappear with moderate fields due to rapid field ionization. We can see from the QCSE picture that this persistence is the result of two factors [10], [20]. First, the wells are sufficiently narrow that even when the particles are pulled to opposite sides of the well, the Coulomb correlation of the electron and hole is still strong; if the wells were made much wider, this would cease to be the case. Second, the electron and hole do not themselves tunnel rapidly out of the wells, thus inhibiting the field ionization that would otherwise broaden the resonance.

The luminescence in wells comparable to those used for absorption has shown behavior explicable through the same QCSE mechanism [31]. Extremely large shifts of the exciton lines were seen in these measurements, with magnitudes in agreement with theory. In addition, for the first time, the luminescence lifetime was directly observed to increase with increasing field, as expected qualitatively from the reduction in the overlap of electron and hole. An approximate quantitative agreement was obtained with the simple overlap integrals in the direction perpendicular to the layers. The magnitude of the luminescence also decreased, presumably for the same reason. In the narrow wells where the lifetime had been observed to decrease with increasing field [17], the tunneling of particles through the barriers is much stronger because the energy of the confined state is higher to start with. In this case, the proposed explanation [17], [23], [40] was that the luminescence is quenched when the particles tunnel through the barriers, a process that can take picoseconds or less. This second mechanism should correlate with broadening of absorption resonances rather than loss of height, although lifetimes have to become quite short for any measurable lifetime broadening (e.g., $< 1$ ps).

Recent theoretical work has also shown the relation between the QCSE electroabsorption and that seen in bulk semiconductors (the Franz–Keldysh effect) [35]. In this work, it is shown in the simplifying limit of negligible excitonic effects that with increasing well thickness, the QW electroabsorption tends smoothly to the Franz–Keldysh effect. For a given field, the change takes place rapidly with thickness, and for a given thickness, Franz–Keldysh behavior dominates once the originally forbidden transitions start to dominate over the "allowed" transitions. In this simplified limit, the QCSE can be described as a quantum-confined Franz–Keldysh effect. This transformation from one behavior to another has not yet been tested experimentally, but the appearance of forbidden transitions is easily observed experimentally [18]. We will also discuss some forbidden transitions below in this paper.

Further measurements of energy shifts were made by

electroreflectance [13], as were other observations of luminescence quenching and other aspects of the luminescence behavior [7]. The absorption properties can also be monitored by photocurrent spectroscopy [20], [32], [34]. Absorption spectroscopy in waveguides [29] enables the two distinct optical polarization directions to be observed, showing preservation of the selection rules with field. We will discuss some of this work in greater detail in this paper. Calculations have been reported of the change in refractive index associated with the electroabsorption [27]. Further calculations of energy level shifts have also appeared [18], [37]. The properties of single particles in a box with field were also considered in other papers [41], [42].

Other modulator devices were demonstrated in GaAs/GaAlAs [12], [24], [28], InGaAs/InGaAlAs [22], InGaAs/InAlAs [26], and GaSb/AlGaSb [33], as were additional SEED configurations [14], [19], [29], and further luminescence devices were proposed [16]. A wavelength-sensitive detector has been demonstrated [25], as has an integrated laser/modulator structure [30]. These devices share a variety of desirable features. For example, they all operate at room temperature, at wavelengths compatible with laser diodes, and with voltages compatible with electronics. They are also very well suited for a variety of optoelectronic integration schemes, given their material compatibility with both electronics and lasers. The electroabsorptive devices also have the advantage of potentially very small size and also very low energy operation compared to other modulation and switching schemes [19]. Both luminescence quenching and electroabsorption may be very fast. Electrical time-constant-limited operation of QCSE modulators has been demonstrated at a $\sim 100$ ps pulse width [28]. The fundamental limit may be much faster. Modulation with a subpicosecond response has been demonstrated for fields parallel to the layers [36], and there is no reason to believe that a slower response should be obtained for the perpendicular field.

In conclusion, as a result of this body of work [3]–[38], a fairly consistent picture of the effects of perpendicular fields on QW optical properties has emerged, encompassing both absorption and luminescence effects. Both of these show device potential, with a large variety of devices demonstrated especially for the absorptive effects.

## III. Waveguide Experiments

Nearly all experiments summarized above were performed using light propagating perpendicular to the quantum well layers. In this section, we give an extended discussion of electroabsorption measurements performed using light propagating parallel to the quantum well layers in a waveguide structure [29]. This geometry is appropriate for planar integrated optoelectronic applications. In addition, it provides a new degree of freedom in that the incident polarization can be either perpendicular or parallel to the quantum well layers. As a consequence, new polarization selection rules are observed. For incident polarization parallel to the plane of the layers, which is the polarization accessible with normal incidence light, both the heavy hole (hh) and light hole (lh) exciton peaks are observed. When the incident polarization is perpendicular to the plane of the quantum well layers, a polarization only accessible in the waveguide geometry, the hh exciton peak disappears and its strength is transferred to the remaining lh exciton peak [43]. This anisotropy is maintained in the presence of large perpendicular electric fields; hence, electrically controllable polarization-sensitive devices are possible using the QCSE.

The long interaction lengths permit studies of samples containing only one or two quantum wells embedded in a waveguide. This structure eliminates the exciton broadening due to field inhomogeneities which occurred in some earlier work [10], [20], resulting in particularly clear spectra. Furthermore, because these are absorption spectra, they can give absolute oscillator strengths not influenced by quantum efficiencies of luminescence or photodetection. Photocurrent spectra often have a field dependence of internal quantum efficiency [20]. These absolute measurements are very important for the verification of the sum rules discussed below. Also, the spectra with $e \| \text{plane}$ offer the unique opportunity to study the lh excitons without the added complication of the hh transitions. This facilitates more quantitative assessments of exciton broadening and absorption strength with field. An additional advantage of the long interaction lengths is that they permit fabrication of modulators and SEED devices with very large on/off ratios which would require prohibitively thick multiple QW growth if the light propagated perpendicular to the layers.

In order to make the samples sufficiently long that they could readily be cleaved to length, yet still transmit some light, we used only two quantum wells centered in a waveguide structure. Due to the symmetric nature of the structure, any light coupled to the higher order guided and radiation modes which have intensity minima at the position of the quantum wells will be only weakly absorbed, and must be eliminated before reaching the detector. Because of this, it is important to limit the higher order guided and radiation modes of the structure in order to obtain accurate absorption measurements. In order to do this, we used a leaky waveguide, designed so that any light coupled to the higher order modes is more strongly attenuated than that coupled to the lowest order mode [43], [44].

The sample (shown in Fig. 1) consisted of two 94 Å thick quantum wells centered in the 3.6 $\mu$m thick superlattice which formed the waveguide core. This was then surrounded by GaAs cladding layers. The use of superlattice rather than the equivalent AlGaAs alloy to form the core of the waveguide offers two advantages: growth of the GaAs layers appears to clean up the impurities that form as a result of the aluminum in the alloy layers, and it improves the electrical characteristics of the devices. Also, it is more convenient to control the refractive index of the superlattice material by varying the relative thick-

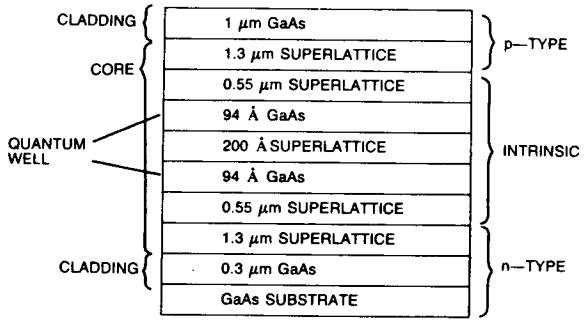


Fig. 1. Sample structure. The superlattice consists of alternate 28 Å GaAs and 50 Å $Al_{0.3}Ga_{0.7}As$ layers. The n and p doping levels are $10^{18}$ $cm^{-3}$ except for the top 0.1 μm of GaAs which is p-doped $10^{19}$ $cm^{-3}$.

nesses of the layers than it is to vary that of AlGaAs by changing the aluminum concentration.

The sample was doped as a p-i-n diode, which could then be reverse biased to apply an electric field to the quantum wells in the intrinsic region. The structure was designed so that a 150 μm long sample would exhibit a 10 dB modulation depth (based on the previous QCSE measurements) and 3 dB attenuation due to the lossiness of the lowest order leaky mode. The maximum loss experienced by the first-order mode should therefore be 13 dB. This is comparable to the 12 dB loss experienced by the second-order mode due to the leaky waveguide losses alone; hence, careful alignment will ensure that the transmitted light due to the coupling to the higher order modes is negligible.

The experiments were performed using an LDS821 dye laser which was pumped by a krypton laser. The beam was spatially filtered and expanded to permit focusing to a near diffraction-limited spot. The light was end fired into and collected from the samples with 6.5 mm focal length laser diode collimating objectives. A portion of the transmitted light was imaged into a television camera to permit observation of the mode structure of the guide.

Fig. 2(a) and (b) show the absorption spectrum at various electric fields for $e\|$plane and $e|$plane, respectively. The zero field spectra exhibit the large polarization anisotropy described earlier. For $e\|$plane, both excitons appear. For $e|$plane, the hh exciton disappears and the lh exciton increases in strength [43].

When a perpendicular electric field is applied, a large shift of the absorption edge to lower energy is seen in both polarizations as a result of the QCSE. The spectra are taken at even higher fields than in some previous multiple QW measurements [20], yet the exciton peaks remain well resolved, the absorption edge remains sharp, and the dichroism persists. The maximum shift observed was 40 meV for the lh exciton with $e|$plane at a field of $2.2 \times 10^5$ V/cm. This is ten times the bulk exciton binding energy and occurs at an applied field 100 times the classical exciton ionization field. Even larger relative shifts have recently been seen in single-well luminescence experiments at low temperature [31]. It is remarkable that at such high fields, the exciton resonances are still clearly resolvable, with very little broadening. These large shifts

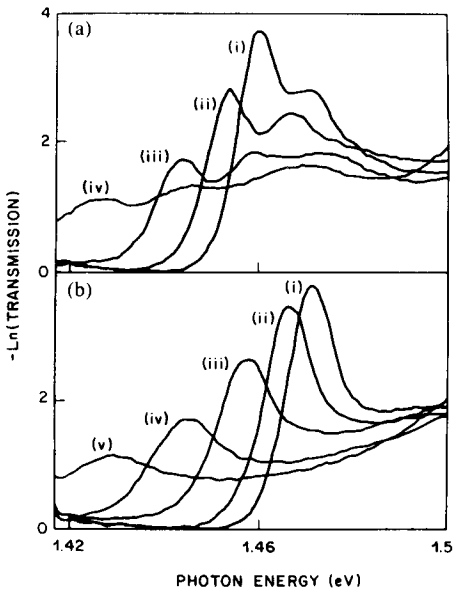


Fig. 2. Absorption spectra of a quantum well waveguide as a function of electric field applied perpendicular to the layers. (a) Incident polarization parallel to the plane of the layers for fields of (i) $1.6 \times 10^4$ V/cm, (ii) $10^5$ V/cm, (iii) $1.3 \times 10^5$ V/cm, and (iv) $1.8 \times 10^5$ V/cm. (b) Incident polarization perpendicular to the plane of the layers for fields of (i) $1.6 \times 10^4$ V/cm, (ii) $10^5$ V/cm, (iii) $1.4 \times 10^5$ V/cm, (iv) $1.8 \times 10^5$ V/cm, and (v) $2.2 \times 10^5$ V/cm. The fields were calculated from $C$-$V$ measurements.

are directly applicable to waveguide devices. Therefore, before discussing the detailed physics of the spectra, we will summarize some of the device results that have been obtained with this sample.

### A. Device Performance

A sample 153 μm long was operated as a modulator by adjusting the laser frequency to just below the exciton absorption edge. With incident photon energies of 1.458 and 1.443 eV for the perpendicular and parallel polarizations, we were able to obtain modulation depths of 10.2 and 9.2 dB, respectively. The measured device insertion loss was $6 \pm 2$ dB, of which 3 dB is due to reflection from the faces. It should be possible to eliminate this with antireflection coatings. Approximately 3 dB is expected due to the leaky waveguides loss. It should be noted, however, that the leaky waveguide was used to overcome the difficulty of coupling a dye laser to a waveguide, whereas actual integrated optical devices could be fabricated as real waveguides and would not suffer this built-in loss. Similar devices from the same material have been demonstrated with modulation down to 100 ps [28].

We have also implemented a number of self-electrooptic effect devices (SEED's) in the waveguide geometry, including optical bistable devices, self-linearized modulators, and optical level shifters. The principle of the SEED [19] is that the device is used simultaneously as a detector and as a modulator. For our measurements, a current source is used to reverse bias the device. The features and analysis of current-biased SEED's are discussed in detail in [19].

Optical bistability was observed when the laser fre-

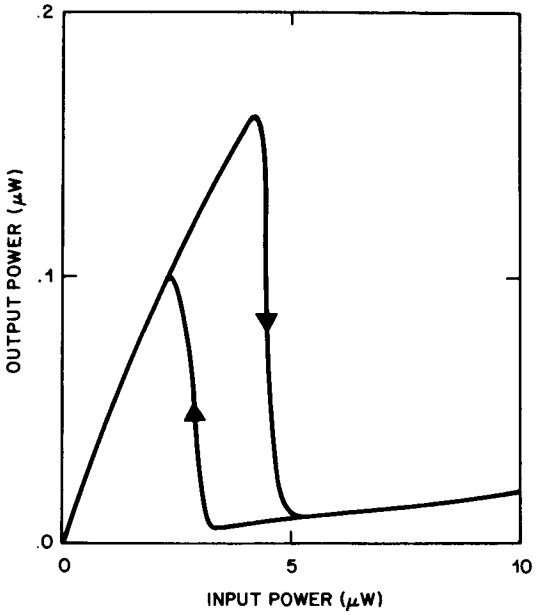


Fig. 3. Measured input/output characteristic at 1.471 eV using a constant current source to bias the device. The incident optical polarization was perpendicular to the layers.

quency was set at or about the zero field exciton position. With no incident light, the exciton peak is shifted to lower energy by the applied bias; with current bias, the entire supply voltage appears across the modulator until the modulator photocurrent exceeds the set current from the bias source. As the incident light intensity increases, the photocurrent produced in the device increases. When the photocurrent exceeds the set current, the voltage across the modulator starts to decrease because the capacitance of the modulator is being dischared, shifting the exciton back towards its zero field energy. This results in increased absorption at the laser frequency, leading to a further increase in the photocurrent, and hence, positive feedback and switching.

We have demonstrated bistability in both polarizations. Fig. 3 shows tha transfer characteristic for $e|$plane, with an incident photon energy of 1.471 eV. We obtained a large on/off ratio of 20:1. This could be increased by either increasing the sample length or adding more wells. Associated with a large on/off ratio is the relatively large background loss seen in these results, although it should be remembered that about 6 dB of the transmission loss is due to avoidable waveguide and reflection losses as discussed above. Due to the large absorption edge shifts that we were able to observe, optical bistability can be observed over a very large range of incident photon energies from 1.455-1.5 eV for $e|$plane and 1.45-1.49 eV for $e\|$plane.

A number of devices can also be demonstrated which make use of negative feedback [14], [19]. These include self-linearized modulation and optical level shifting. A constant current source is again used to bias the device; however, the incident photon energy is set to below the zero field exciton energy. In this configuration, an increased bias voltage results in increased absorption. The operating principle of these devices is that the photocurrent is proportional to the absorbed light intensity, and this condition is stabilized by negative feedback. If the photocurrent is less than the set current, then the current source increases the voltage on the device. This shifts the exciton to lower energy, increasing the absorption, which increases the photocurrent until it equals the set current. If the photocurrent is greater than the set current, then the opposite occurs. The photocurrent is related to the absorption by the internal quantum efficiency, which is empirically constant over a large voltage range; hence, the power absorbed by the device depends linearly on the set current. The transmitted light power is therefore shifted by an amount proportional to the set current. This is shown in Fig. 4. The device is operated as a self-linearized modulator by modulating the set current to linearly modulate the absorbed energy. This is shown in Fig. 5. The chief advantage of this device over previous MQWS devices is the large dynamic range of modulation and level shifting due to the long optical path length.

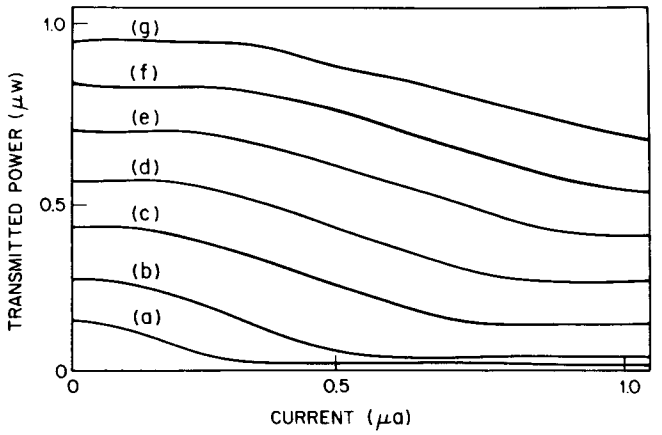


Fig. 4. Optical output power as a function of current at a photon energy of 1.452 eV and with incident polarization perpendicular to the plane of the layers. The incident optical powers are (a) 1, (b) 1.8, (c) 3, (d) 4.2, (e) 5.4, (f) 6.6, and (g) 7.7 μW, respectively.

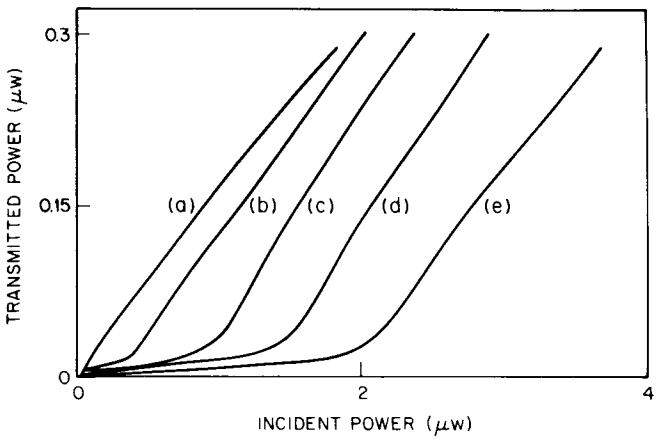


Fig. 5. Transmitted optical power versus incident optical power under constant current bias with currents of (a) 0, (b) 0.125, (c) 0.25, (d) 0.375, and (e) 0.5 μA, respectively. The incident photon energy is 1.452 eV and the incident polarization is perpendicular to the plane of the layers.

TABLE I
PARAMETERS FOR SPECTRA WITH $e$|PLANE

| Normalized Area[a] | Width (meV) | Shift (meV) | Voltage | Delta HWHM Exp. (meV) | Delta HWHM Theor. (meV) | Adjusted Field (V/cm) | $C$-$V$ Field (V/cm) |
|---|---|---|---|---|---|---|---|
| 1.00 | 5.9 | 0 | 0 | 0 | 0 | 0 | $1.6 \times 10^4$ |
| 1.03 | 5.9 | −5 | 10 | 0 | 0.07 | $6 \times 10^4$ | $1.0 \times 10^5$ |
| 1.01 | 7.0 | −14 | 15 | 1.1 | 0.19 | $1.1 \times 10^5$ | $1.4 \times 10^5$ |
| 0.98 | 8.0 | −26.5 | 20 | 2.1 | 0.45 | $1.5 \times 10^5$ | $1.8 \times 10^5$ |
| 0.94[b] | 9.9[b] | −43 | 25 | 4[b] | 0.92 | $2.0 \times 10^5$ | $2.2 \times 10^5$ |

[a] This is the area under the absorption spectrum between 1.42 and 1.5 eV.
[b] Note that the absorption is still significant at 1.42 eV for this spectrum, so that the width measurement is less accurate and there is some area missing from the spectrum at low energies.

### B. Analysis of Spectra

The spectra in Fig. 2 show a number of features that are interesting to compare to experiment. First, it has not previously been possible in absorption measurements to compare the broadening of the peaks with field to theory because of large field inhomogeneities in multiple well samples and the overlapping of light and heavy hole features [20]. A better comparison should be possible here. Second, for the same reasons, it should also be possible to compare detailed models of the variation of absorption strength with field to experiment.

The first stage in comparing theory to experiment is the calculation of energy levels and wavefunctions. We have chosen to do this by the tunneling resonance technique [20]. This simple numerical technique automatically includes the effects of finite barrriers and, as extended by us here, yields energy levels, wavefunctions, and broadenings for the single-particle states. The technique involves looking at the transmission of the structure (usually a single well and two barriers) as a function of the energy of the incident particle wave. The effect of electric field is included by sloping the whole structure uniformly. The transmission is calculated by dividing the structure up into a number of uniform layers and evaluating the forward and backward waves at each interface. The resonances in transmission correspond to the energy levels of the system, and a good representation of the "eigen" functions is obtained from the steady-state standing wave pattern in this transmission problem. There are, of course, no true eigenfunctions of this system as there are strictly no bound states, and the lifetimes in this method are given by the widths of the resonances. This particular method is analogous to evaluating the modes of an optical Fabry–Perot resonator in a transmission experiment; the relation between different methods of solving this problem have been discussed [44], with all methods being essentially equivalent if the finesse of the resonator is large enough. To evaluate overlap integrals by this method, we arbitrarily truncate the wavefunctions halfway through the barriers and normalize them; when the resonance is narrow, the amplitude of the wavefunction is negligible beyond this point anyway. As before [20], we can include excitonic effects by presuming that the wavefunction is separable and solving for the best 1$S$-like wavefunction in the plane of the layers using variational techniques.

In our calculations, the energies of the exciton peaks were obtained by adding the valence and conduction subband energies, evaluated by the tunneling resonance technique, to the GaAs bandgap of 1.424 eV and then subtracting from this the exciton binding energies, which were calculated variationally [20].

The electric field in the intrinsic region was determined from measurements of capacitance versus voltage ($C$-$V$). The $C$-$V$ measurements indicated that the depletion region extended through the intrinsic region even at 0 V; however, the experimental energy shifts were found to be somewhat less than predicted. It was possible to obtain good agreement between theory and experiment by subtracting approximately 3.5 V from the data. In conjunction with this, the overall responsivity in photocurrent spectra was observed to increase for voltages up to 3.5 V, remaining constant for higher voltages (apart from the field-induced changes in the form of the spectra). We have observed this behavior in several samples with a variety of different offset voltages, but always with a strong correlation between the voltage at which the overall responsivity levels off and the start of field-induced shifts in the spectra. The mechanism for this offset is not clear, but it appears to be wafer dependent. As a result of this discrepancy in the electric field, we will discuss our experimental results in terms of the fields that we deduce from the exciton peak shifts because we believe these to be the best representation of the effective electric field at the quantum well. These fields are quoted as the adjusted fields in Table I.

To provide a quantitative basis for analyzing the spectra, the parameters of width and area for the lh exciton quoted in Table I were determined by fitting the spectra using a semi-empirical model consisting of a Gaussian and a Sommerfeld broadened continuum to represent the lh exciton and band-to-band transitions, respectively. This kind of model, although it has little *a priori* justification, has been used successfully to model changes excitonic behavior in QW's [45]. The lifetime broadening of the exciton peaks was calculated using the tunneling resonance model previously described, under the assumption that the excitons only ionize when the carriers tunnel out of the

wells. A 60:40 percent conduction : valence band discontinuity ratio was assumed. Using these calculation and analysis methods, we will now attempt to analyze the spectra. As we will discuss, some of the features can be well explained by these methods, but others require further work; some of these others can be described by use of sum rules, and we will postpone their detailed discussion until Section IV.

*1) Exciton Broadening:* The experimental and theoretical lh exciton broadening are shown in Table I. One caution in interpreting these broadening data is that it is not clear how to convolve the different contributions to the linewidth. There is, for example, no particular reason simply to add the linewidth contributions linearly; this point has been discussed in [20]. Although the broadening is less than in the case of the MQW's [20], it is still somewhat more than that predicted even using a simple linear addition of linewidths (other methods of adding linewidths such as the sum of squares method would give even greater disagreement). This may be due to inhomogeneous broadening results from variations in the electric field along the length of the layers. Also, the tunneling rate for light holes is very sensitive to the conduction band-valence band offsets, which are still not definitively established. Another possible reason is the growth of unresolved forbidden transitions to other excitonic states. We will discuss this possibility below in Section IV. The precise mechanism of the broadening still is unclear, however.

*2) Interband Absorption Strength:* In Fig. 2, a considerable loss of oscillator strength in the lh band-to-band and excitonic transitions is observed as the electric field is increased. In the case of absorption well above the excitonic peak, the simplest approximation is to presume that we may neglect any perturbation of the electron and hole wavefunctions in the plane of the layers; then the overlap integral is porportional to the overlap of the wavefunctions in the direction perpendicular to the layers. With this simplification, the loss of interband absorption is the result of the decreased overlap of the electron and hole wavefunctions perpendicular to the layers as they are pulled to opposite sides of the well. This is the theoretical approach taken by some previous authors [5], [31]. We have calculated the electron–hole overlap given by $|\langle \phi^e | \phi^h \rangle|^2$ for the various transitions as a function of electric field. Here $|\phi^e\rangle$ and $|\phi^h\rangle$ are the electron and hole $z$ wavefunctions determined from tunneling resonance calculations. These calculations are simplified compared to the case of MQW's at normal incidence since we only need include the lh wavefunctions. For comparison to this, the band–band absorption was measured at a point 20 meV above the lh exciton energy. These results are plotted in Fig. 6 as a function of exciton shift. Excellent agreement is seen.

*3) Exciton Peak Height and Area:* The circles in Fig. 7 represent the lh exciton height versus exciton peak energy shift. The exciton height clearly decreases faster than the overlap integral (solid curve). This is expected on two

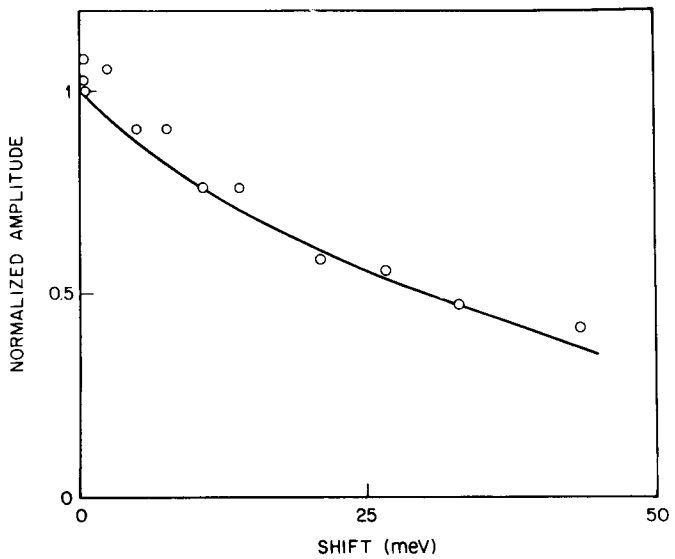


Fig. 6. The circles represent the light hole continuum height versus exciton shift, normalized to the zero shift height. The solid line is the squared electron–hole overlap integral.

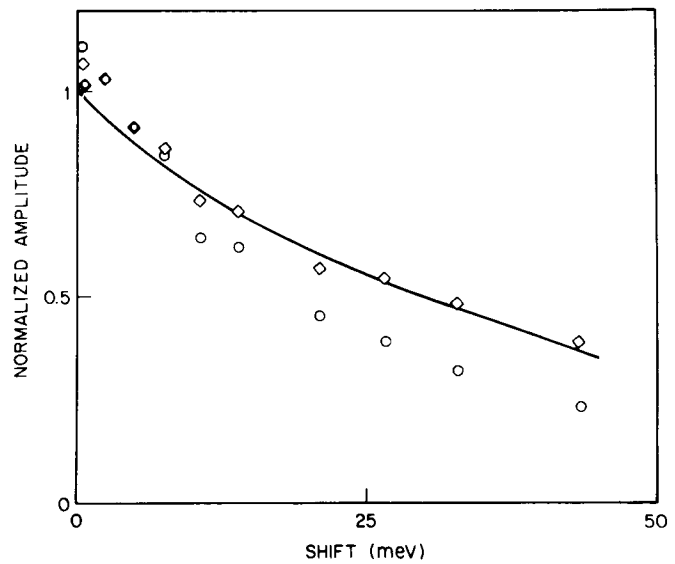


Fig. 7. The circles and diamonds represent, respectively, the experimental light hole exciton height and integrated area versus exciton shift. The solid line is the squared electron–hole overlap integral.

grounds: first, the exciton wavefunction in the plane of the layers is expected to become larger with increasing field because of the reduced Coulomb interaction between the separated electron and hole; second, the exciton peak is expected to broaden with field, and this should decrease the height of the peak as it broadens it. The diamonds in Fig. 7 represent the lh exciton integrated area as determined from our semi-empirical fitting procedure. Certainly, we find that the exciton integrated area follows the overlap integral quite well, in agreement with a broadening. However, some care is required here due to the fact that the simple broadening measurement does not agree with theory, and other forbidden transitions may be coming into play. We will discuss this point again after deriving the sum rules.

*4) Forbidden Transitions:* For the parallel polarization in which both lh and hh excitons are observed, a third peak appears in the spectra at high electric fields. This effect has been seen in [20], and we ascribe it here to the $n = 1$ conduction band to $n = 2$ hh transition. This transition is normally forbidden by symmetry at zero field. At $1.5 \times 10^5$ V/cm, corresponding to curve (iv) in Fig. 2(a), the overlap integral is 0.44 and the theoretical energy is 1.473 eV, in good agreement with experiment insofar as this can be deduced from the spectra with both lh and hh transitions. This behavior also itself suggests a sum rule because it can be seen in Fig. 2(a) that the absorption above this transition is changed relatively little by the field; again, we will return to this point after deriving the sum rules.

*5) Overall Absorption Conservation:* We also point out the appearance of an empirical sum rule in our spectra. We have calculated the total absorption integrated over the entire spectral range shown in Fig. 2 in both polarizations. This is listed for the perpendicular polarization in Table I. We find that the integrated absorption in both polarizations is independent of applied field to within our experimental error. We will return to this in Section IV.

## IV. Sum Rules for Electroabsorption

In this section, we will derive simple sum rules for absorption near the bandgap with applied electric field. First, we will briefly derive the general expression for the absorption including excitonic effects. The derivation is relatively standard (see, for example, [46]), except that it is done without solving for the actual excitonic behavior, and we summarize it to introduce the necessary approximations explicitly and to show why it remains valid in the presence of fields and quantum confinement. We also extend it to the case of separable wavefunctions, which are a useful approximation for quantum wells. Second, we will derive the necessary mathematical identities for the sum rules; these follow from the completeness and orthonormality of sets of eigenfunctions. Third, we will derive three sum rules, and finally, we will compare these to experiment.

### A. Optical Absorption for Creation of an Electron–Hole Pair

Consider the set of excited states of the crystal $|\Psi_{n,\boldsymbol{K}}\rangle$ corresponding to one electron in the conduction band and one hole in the valence band(s) where these states are the eigenstates of some Hamiltonian $H$, i.e.,

$$\mathrm{H}|\Psi_{n,\boldsymbol{K}}\rangle = E_{n,\boldsymbol{K}}|\Psi_{n,\boldsymbol{K}}\rangle. \tag{1}$$

Because they are eigenstates, $|\Psi_{n,\boldsymbol{K}}\rangle$ form a complete set, a fact that is important for the sum rules. We choose two quantum numbers, $n$ and $\boldsymbol{K}$, to label the state. $\boldsymbol{K}$ is the center-of-mass wavevector, and we will presume that it is a constant of the motion because the center-of-mass is not perturbed by either the electron–hole interaction (as in the usual exciton case) or by any uniform fields as the electron–hole pair has no net charge. We will also assume that $|\Psi_{n,\boldsymbol{K}}\rangle$ can be expanded in Slater determinants $|\Phi_{k_e,k_h,m}\rangle$ of Bloch functions corresponding to an electron in the conduction band with wavevector $\boldsymbol{k}_e$ and a hole in valence band $m$ with wavevector $\boldsymbol{k}_h$. We will consider spin to be included within the indexing in $\boldsymbol{k}_e$ and $\boldsymbol{k}_h$. We can write, therefore,

$$|\Psi_{n,\boldsymbol{K}}\rangle = \sum_m \sum_{\boldsymbol{k}_e} A_{n,\boldsymbol{k}_e,\boldsymbol{k}_e-\boldsymbol{K},m}|\Phi_{\boldsymbol{k}_e,\boldsymbol{k}_e-\boldsymbol{K},m}\rangle \tag{2}$$

where $\boldsymbol{K} = \boldsymbol{k}_e - \boldsymbol{k}_h$ to give the chosen center-of-mass motion. The ground state of the crystal is presumed to be the Slater determinant $|\Phi_o\rangle$ corresponding to full valence bands. The use of Slater determinants is a simplification in the case of quantum well material since the crystal is no longer truly periodic with unit cell periodicity, but this will not concern us further. We also neglect any nonlocal response in the quantum well, assuming that the wavelength of light is much longer than the thickness of the layers, averaging the response over the layers.

Even though we may not know the solutions $|\Psi_{n,\boldsymbol{K}}\rangle$, we can still proceed to derive the sum rules for optical absorption. By the standard results of time-dependent perturbation theory, we may write for the transition rate $W_{n,\boldsymbol{K}}$ from the ground state $|\Phi_o\rangle$ to the excited state $|\Psi_{n,\boldsymbol{K}}\rangle$

$$W_{n,\boldsymbol{K}} = 2\pi\hbar \frac{e^2A_0^2}{m_o^2} |M_{n,\boldsymbol{K}}|^2 \, \delta(E_{n,\boldsymbol{K}} - E_o - \hbar\omega) \tag{3}$$

where the vector potential is

$$\boldsymbol{A} = \hat{\boldsymbol{e}}A_0 \exp(i[\boldsymbol{q}\cdot\boldsymbol{r} - \omega t]) + \text{c.c.}$$

and

$$M_{n,\boldsymbol{K}} \equiv \langle\Psi_{n,\boldsymbol{K}}|\hat{\boldsymbol{e}}\cdot\nabla|\Phi_o\rangle.$$

We have presumed the optical wavevector $\boldsymbol{q}$ to be negligibly small as usual, and we have neglected the emission term in $W_{n,\boldsymbol{K}}$.

To evaluate $M_{n,\boldsymbol{K}}$, we define the Fourier transform of $A_{k_c,k_c-\boldsymbol{K},m}$ in $\boldsymbol{k}_c$ as

$$U_{n,\boldsymbol{K}}(\boldsymbol{r}) = \frac{1}{\sqrt{N}} \sum_m \sum_{\boldsymbol{k}_c} A_{n,\boldsymbol{k}_c,\boldsymbol{k}_c-\boldsymbol{K},m} \exp(i\boldsymbol{k}_c\cdot\boldsymbol{r}) \tag{4}$$

where $\boldsymbol{r}$ is now the electron–hole relative position vector. $N$ is the number of unit cells in the crystal. (Note that overall normalization of the two-particle wavefunction is preserved because another $1/\sqrt{N}$ appears in the rest of the wavefunction [46] for center-of-mass motion.) Considering only allowed transitions, we find finite $M_{n,\boldsymbol{K}}$ only for $\boldsymbol{K} = 0$ as usual. Henceforth, we drop the $\boldsymbol{K}$ index and, using $U_n(O) \equiv (1/\sqrt{N})\,\Sigma_m\,\Sigma_{k_c} A_{n,k_c,k_c,m}$ obtain

$$M_n = \frac{im_o}{2\hbar} PU_n(O). \tag{5}$$

Here $P$ is the momentum matrix element $(2/m_o)$ $\langle u_c|-i\hbar e\cdot\nabla|u_v\rangle$ between the conduction and valence unit cell wavefunctions $u_c$ and $u_v$, assumed independent of $\boldsymbol{k}_e$. $m_o$ is the free electron mass. Note that we have presumed that $P$ is the same for all valence bands of interest. This is valid for bands that are degenerate in en-

ergy at zone center. In quantum wells, $P$ is also the same for all the subbands which originate from the same bulk band and form a set of "confinement shifted" energy levels with otherwise the same properties. We will also average over all polarization directions, introducing a factor of $\frac{1}{3}$ after squaring the matrix element as usual. This averaging procedure deserves some comment owing to the very special structure of the valence subband in III–V compound quantum wells. Within the effective mass approximation, the effect of the confinement has the same symmetry as a uniaxial stress and lifts the degeneracy of the $J = \frac{3}{2}$ bulk valence band. The uppermost valence subband of QW's consist of the heavy hole (hh) subband ($J = \frac{3}{2}$, $M = \pm\frac{3}{2}$) and the light hole subband (lh). The optical transitions have to obey the selection rules imposed by the conservation of angular momentum. The normalized transition probabilities are in the ratio 3/4 and 1/4 for $E$ parallel to the plane of the layers, respectively, for the transitions hh and lh to the conduction band. For $E$ normal to the layers, they are 0 and 1 so that the average over the three directions is the same for the two polarizations.

Summing over all possible transitions, we therefore obtain for the optical absorption coefficient $\alpha(\hbar\omega)$

$$\alpha(\hbar\omega) = B \sum_n |U_n(O)|^2 \, \delta(E_n - E_o - \hbar\omega) \tag{6}$$

where $B$ is given by

$$B = \frac{\pi e^2 |P|^2}{3 m_o c \epsilon_o \omega \eta V}$$

where $V$ is the volume of the crystal and $\eta$ is the refractive index. This is a standard result, but in our case is made without explicit knowledge of the nature of the $U_n(r)$.

One particular form of electron–hole wavefunction that will be of interest to us is that in which the motion separates into electron and hole motion in the $z$ direction (i.e., perpendicular to the layers), with electron and hole coordinates $z_e$ and $z_h$ and separable center-of-mass motion (as before) in the $x$ and $y$ directions (i.e., in the plane of the layers). Such a separable wavefunction is an approximation, but has been successfully used in calculating exciton binding energies and enables us to derive other sum rules in the case of strong quantization. In this case, we repeat the above derivation, considering instead of (1) the equivalent expansion

$$|\Psi_{l,q,s,\boldsymbol{K}_{xy}}\rangle = \sum_m \sum_{k_{ze}} \sum_{k_{zh}} \sum_{\boldsymbol{k}_{xy}} A_{l,q,s,k_{ze},k_{he},\boldsymbol{k}_{xy},\boldsymbol{k}_{xy}-\boldsymbol{K}_{xy},m} \, |\Phi_{k_{ze},k_{zh},\boldsymbol{k}_{xy}-\boldsymbol{K}_{xy},m}\rangle \tag{7}$$

where $k_{ze}(k_{zh})$ is the electron (hole) wavevector in the $z$ direction and $\boldsymbol{k}_{xy}$ ($\boldsymbol{K}_{xy}$) is the relative (center-of-mass) electron–hole wavevector in the $xy$ plane. $l$, $q$, and $s$ are quantum numbers for the $z_l$, $z_h$, and $\boldsymbol{r}_{xy}$ (electron–hole relative $xy$ position) motion.

As before (4), we Fourier transform now in $k_{ze}$, $k_{zh}$, and $\boldsymbol{k}_{xy}$ to obtain

$$U_{l,q,s,\boldsymbol{K}}(z_l, z_h, \boldsymbol{r}_{xy}) = \frac{1}{\sqrt{M}} \sum_{\boldsymbol{k}_{xy}} \frac{1}{\sqrt{Q}} \sum_{k_{ze}} \frac{1}{\sqrt{Q}} \sum_{k_{zh}} \sum_m \cdot A_{l,q,s,k_{ze},k_{zh},\boldsymbol{k}_{xy},\boldsymbol{k}_{xy}-\boldsymbol{K}_{xy},m} \times \exp\,[i(k_{ze} z_l + k_{zh} z_h + \boldsymbol{k}_{xy}\boldsymbol{r}_{xy})]. \tag{8}$$

$M$ is the number of unit cells in the plane and $Q$ is the number perpendicular to the layers, so that $N = MQ$; these factors are necessary to preserve normalization of the wavefunction. (Another factor of $1/\sqrt{M}$ will come from the rest of the wavefunction describing the $xy$ center-of-mass motion.) Now we presume a separable form for $U$:

$$U_{l,q,s,\boldsymbol{K}}(z_e, z_h, \boldsymbol{r}_{xy}) = \phi_l^e(z_e) \, \phi_q^{h^*}(z_h) \, \psi_{s,\boldsymbol{K}_{xy}}(\boldsymbol{r}_{xy}). \tag{9}$$

This can be achieved, in general, if

$$\sum_m A_{l,q,s,k_{ze},k_{zh},\boldsymbol{k}_{xy},\boldsymbol{k}_{xy}-\boldsymbol{K}_{xy},m} \equiv a_{l,k_{ze}} \left[\sum_m b^*_{q,k_{zh},m}\right] \left[\sum_m C_{s,\boldsymbol{k}_{xy},\boldsymbol{k}_{xy}-\boldsymbol{K}_{xy},m}\right] \tag{10}$$

and the separated wavefunctions are normalized if

$$\phi_l^e(z_e) = \frac{1}{\sqrt{Q}} \sum_{k_{ze}} a_{l,k_{ze}} e^{ik_{ze}z_e}$$

$$\phi_q^h(z_h) = \frac{1}{\sqrt{Q}} \sum_m \sum_{k_{zh}} b_{q,k_{zh},m} e^{ik_{zh}z_h}$$

$$\psi_{s,\boldsymbol{K}_{xy}}(\boldsymbol{r}_{xy}) = \frac{1}{\sqrt{M}} \sum_m \sum_{\boldsymbol{k}_{xy}} C_{s,\boldsymbol{k}_{xy},\boldsymbol{k}_{xy}-\boldsymbol{K}_{xy},m} e^{i\boldsymbol{k}_{xy}\cdot\boldsymbol{r}_{xy}}. \tag{11}$$

Now we consider the matrix element

$$M_{l,q,s,\boldsymbol{K}_{xy}} \equiv \langle \Psi_{l,q,s,\boldsymbol{K}_{xy}} | \hat{\boldsymbol{e}} \cdot \nabla | \Phi_0 \rangle.$$

As before, we now find that only those transitions with $k_{ze} = k_{zh}$ and $\boldsymbol{K}_{xy} = 0$ survive to give

$$M_{l,q,s} = \frac{i m_o}{2\hbar} P \left[\left(\frac{1}{\sqrt{Q}}\right)^2 \sum_m \sum_{k_z} a^*_{l,k_z} b_{q,k_z,m}\right] \cdot \frac{1}{\sqrt{M}} \sum_m \sum_{\boldsymbol{k}_{xy}} C_{s,\boldsymbol{k}_{xy},\boldsymbol{k}_{xy},m} \tag{12}$$

where again we have dropped the index $\boldsymbol{K}_{xy}$. Now

$$\langle \phi_l^e | \phi_q^h \rangle \equiv \left(\frac{1}{\sqrt{Q}}\right)^2 \sum_z \sum_m \sum_{k_{zl}} \sum_{k_{zh}} a^*_{l,k_{zl}} b_{q,k_{zh}} e^{i(k_{zh}-k_{ze})z} = \left(\frac{1}{\sqrt{Q}}\right)^2 \sum_m \sum_{k_z} a^*_{l,k_z} b_{q,k_z,m} \tag{13}$$

(where $\Sigma_z$ is the sum over all unit cells) and

$$\frac{1}{\sqrt{M}} \sum_m \sum_{\boldsymbol{k}_{xy}} C_{s,\boldsymbol{k}_{xy},\boldsymbol{k}_{xy},m} = \psi_s(0). \tag{14}$$

So

$$\alpha(\hbar\omega) = B \sum_l \sum_q \sum_s |\langle \phi_l^e | \phi_q^h \rangle|^2 \, |\psi_s(0)|^2 \times \delta(E_l + E_q + E_s - E_0 - \hbar\omega) \tag{15}$$

where $E_l$, $E_q$, and $E_s$ are the eigenenergies associated with the states $l$, $q$, and $s$ in the separated problems.

### B. Derivation of Mathematical Identities for Sum Rules

Consider first two complete orthonormal sets $A_m(\boldsymbol{x})$ and $B_n(\boldsymbol{x})$ spanning the same space. (This space may be one dimensional, two dimensional, three dimensional, or any other appropriate space.) We may expand one in terms of the other, i.e.,

$$A_m(\boldsymbol{x}) = \sum_n a_{mn} B_n(\boldsymbol{x}) \tag{16}$$

where, by orthonormality,

$$a_{mn} = \int B_n^*(\boldsymbol{x})\, A_m(\boldsymbol{x})\, d\tau_x = \langle B_n | A_m \rangle \tag{17}$$

with $\tau_x$ being the element of volume in the space. Also by orthonormality, we have

$$\int A_j^*(\boldsymbol{x})\, A_q(\boldsymbol{x})\, d\tau_x = \langle A_j | A_k \rangle = \delta_{jq} \tag{18}$$

and, by substituting for $A_j^*(\boldsymbol{x})$ using (16),

$$\sum_l a_{jl}^* a_{ql} = \delta_{jq} \tag{19a}$$

or using $B$ instead of $A$ throughout,

$$\sum_l a_{lj}^* a_{lq} = \delta_{jq}. \tag{19b}$$

We wish to evaluate sum rules for absorption, and these will involve terms like $\Sigma_q |A_q(0)|^2$. However, such a sum does not converge. Instead, we will consider the difference of two such sums, which will correspond to the difference in the integrated absorption in two cases. Hence, we consider

$$S = \sum_q |A_q(0)|^2 - \sum_l |B_l(0)|^2. \tag{20}$$

Substituting for $A_m(0)$ from (16), we find

$$S = \sum_n \sum_p B_n^*(0)\, B_p(0) \sum_m a_{mn}^* a_{mp} - \sum_l |B_l(0)|^2. \tag{21}$$

Without loss of generality, we may choose $n = l$. Using (19), we therefore obtain

$$S = \sum_n \left[ \sum_p B_n^*(0)\, B_p(0)\, \delta_{np} - |B_n(0)|^2 \right]. \tag{22}$$

Although the sums of the individual terms may not converge, we have identical term-by-term cancellation, and so

$$S = 0. \tag{23}$$

Therefore, using only completeness and orthonormality, we have proved a simple sum rule that will form the basis for our excitonic absorption sum rules below.

To derive a second simple identity, consider again the two complete orthonormal sets. From (16),

$$\langle A_m | A_m \rangle = \sum_n |a_{mn}|^2. \tag{24}$$

Using the normalization condition for $A_m(\boldsymbol{x})$ and the definition (17), we therefore obtain

$$\sum_n |\langle B_n | A_m \rangle|^2 = 1. \tag{25}$$

This will form the basis for a sum rule on the heights of the "steps" in the quantum well absorption spectrum.

### C. Sum Rules

In all the sum rules that follow, we will treat $B$ of (6) and (15) as a constant, neglecting its slow variation with $\omega$ over the spectral range that interests us and also neglecting variations in refractive index.

We consider first the case where we have made no assumption of separability. Suppose that under one set of conditions (e.g., no applied field), the electron–hole relative position eigenfunctions are $U_n^i(\boldsymbol{r})$ and under another set of conditions (e.g., with applied field) and $U_m^f(\boldsymbol{r})$. Both of these sets are complete as they are the sets of eigenfunctions of Hamiltonians $H_0$ and $H_f$, respectively, operating on the same Hilbert space. The integral over photon energy of the difference in the two absorption coefficients ($\alpha_0(\hbar\omega)$ and $\alpha_f(\hbar\omega)$, respectively) is, from (6),

$$\begin{aligned}\Delta A &\equiv \int [\alpha_i(\hbar\omega) - \alpha_0(\hbar\omega)]\, d\hbar\omega \\ &= B\left[ \sum_m |U_m^f(0)|^2 \int \delta(E_m - E_0 - \hbar\omega)\, d\hbar\omega \right. \\ &\qquad \left. - \sum_n |U_n^i(0)|^2 \int \delta(E_n - E_0 - \hbar\omega)\, d\hbar\omega \right] \\ &= B\left[ \sum_m |U_m^f(0)|^2 - \sum_n |U_n^i(0)|^2 \right]\end{aligned} \tag{26}$$

provided only that the range of integration is large enough to encompass all $E_m$ and $E_n$. Hence, using the identity (23), we obtain

$$\text{sum rule 1: } \Delta A = \int_0^\infty [\alpha_i(\hbar\omega) - \alpha_0(\hbar\omega)]\, d\hbar\omega = 0. \tag{27}$$

This is a very general sum rule, and the principal restriction is one made at the beginning of this whole derivation, that we assume the center-of-mass motion is uniform, with $\boldsymbol{K}$ as a constant of the motion for both $H_0$ and $H_f$. This is satisfied for electron–hole Coulomb interaction and for the consequences of uniform electric fields in any direction. It should therefore apply to the specific case that we will discuss below in this paper for perpendicular fields in quantum wells (the QCSE), and also to the cases of parallel fields in quantum wells, fields in any direction in bulk materials, and applies whether or not the electron–hole interaction is considered. It also therefore applies to the Franz–Keldysh effect and the quantum-confined Franz–Keldysh effect [35]. It is also valid for structures other than a simple quantum well, such as superlattices or other single or multiple layer structures.

Now we consider the case where we presume that we may separate the wavefunction as in (9). This is relevant when the confinement energy is large compared to the strength of the electron–hole Coulomb interaction. The $z$ motions of electron and hole can be solved separately, neglecting the coupling between them for this direction, and the coupling can be reintroduced into the problem to solve for the $xy$ relative motion. If this is done, the $xy$ relative motion eigenfunctions $\psi_s(r_{xy})$ form a complete set spanning the two-dimensional $xy$ space, and the electron and hole wavefunctions in the $z$ direction, $\phi_l^e(z_e)$ and $\phi_q^h(z_h)$, also each form complete sets spanning the one-dimensional $z$ space. Note that for each $l$ and $q$, the Hamiltonian for the $xy$ motion [and hence the $\psi_s(r_{xy})$] may be different as the $z$ charge distribution may be different in each case, thus affecting the form of the electron–hole Coulomb terms in the $xy$ plane; this will not invalidate our sum rules. To demonstrate this (and to avoid confusion), we explicitly include indexes $l$ and $q$ on $\psi_s$, e.g., $\psi_s(r_{xy}) \rightarrow \psi_{lqs}(r_{xy})$. $\psi_{lqs}(r_{xy})$ is still a complete set of wavefunctions spanning the $xy$ space.

Proceeding as above, we define the various complete sets of functions under one set of conditions as $\phi_l^{eo}(z_e)$, $\phi_q^{ho}(z_h)$ and $\psi_{lqs}^o(r_{xy})$ and under another set of conditions as $\phi_m^{ef}(z_e)$, $\phi_p^{hf}(z_h)$ and $\psi_{mpt}^f(r_{xy})$. Consider first the case of absorption $\alpha_{lq}$ due to transitions between subband $q$ in the valence band and subband $l$ in the conduction band. Let us presume that above some energy $\Delta E_{\max}$ (corresponding to an index $t > t_{\max}$) above the lowest transition energy $E_{lqf}$ or $E_{lqo}$ between these subbands, the states $\psi_{lqt}^f$ and $\psi_{lqt}^o$ are essentially identical, being negligibly perturbed.

$$\begin{aligned}\Delta A_{lq} &= \int_{E_{lqf}}^{E_{lqf}+\Delta E_{\max}} \alpha_{lqf}(\hbar\omega)\, d\hbar\omega \\ &\quad - \int_{E_{lqo}}^{E_{lqo}+\Delta E_{\max}} \alpha_{lqo}(\hbar\omega)\, d\hbar\omega \\ &= B\Big\{ |\langle\phi_l^{ef}|\phi_q^{hf}\rangle|^2 \sum_{t=0}^{t_{\max}} |\psi_{lqt}^f(0)|^2 \\ &\quad - |\langle\phi_l^{eo}|\phi_q^{ho}\rangle|^2 \sum_{t=0}^{t_{\max}} |\psi_{lqt}^o(0)|^2 \Big\}. \end{aligned} \tag{28}$$

However, since we are presuming that $\psi_{lqt}^f$ and $\psi_{lqt}^o$ are identical for $t \geq t_{\max}$,

$$\sum_{t=t_{\max}}^{\infty} [|\psi_{lqt}^f(0)|^2 - |\psi_{lqt}^o(0)|^2] = 0 \tag{29}$$

and hence, using (23),

$$\sum_{t=0}^{t_{\max}} |\psi_{lqt}^f(0)|^2 = \sum_{t=0}^{t_{\max}} |\psi_{lqt}^o(0)|^2 \tag{30}$$

so that

sum rule 2: $\Delta A_{lq}$

$$= B \sum_{t=0}^{t_{\max}} |\psi_{lqt}^o(0)|^2 [|\langle\phi_l^{ef}|\phi_q^{hf}\rangle|^2 - |\langle\phi_l^{eo}|\phi_q^{ho}\rangle|^2]. \tag{31}$$

In other words, provided that $\Delta E_{\max}$ is sufficiently large, the total absorption within the first $\Delta E_{\max}$ on a given set of intersubband transitions is proportional to the square of the $z$ overlap integral, independent of the detailed form of the $xy$ wavefunctions.

This sum rule will apply to the case of a quantum well with confinement strong compared to the Coulomb energy so that we can consider there to be separate excitons associated with each valence subband to conduction subband absorption. It states, in effect, that if we integrate over the excitonic absorption up to a sufficiently high energy, the resulting total absorption scales with the $z$ overlap and is independent of the nature of any changes in the $xy$ orbital motion.

Another very simple sum rule follows directly from (25). Consider for the moment the limit where we neglect any interaction between electron and hole. The $xy$ motion then becomes plane waves and is decoupled from the $z$ motion even in the presence of field in the $z$ direction. The optical absorption then reduces to a set of steps whose heights are proportional to $|\langle\phi_{el}|\phi_{hq}\rangle|^2$. Suppose now that we consider all the transitions between a given, say, conduction subband and all the hole subbands corresponding to a particular kind of hole, say, heavy hole. The total height of steps corresponding to all these transitions, in dimensionless units, is

$$\text{sum rule 3: } \sum_q |\langle\phi_{el}|\phi_{hq}\rangle|^2 = 1 \tag{32}$$

by (25) where we presume only that $\phi_{el}$ and $\phi_{hq}$ are complete orthonormal sets spanning the same space. A similar rule applies to electrons in the case of an infinitely deep well at zero field, the two sets of functions $\phi_{el}$ and $\phi_{hq}$ are geometrically identical, and only the step $l = q$ survives. This (third) sum rule tell us that when the system is perturbed by, for example, electric field, the sum of the step heights for all of these transitions will come to the same height as that of the single unperturbed step. Note that it is not possible for a step to "grow" to a height greater than 1 in the units of (32) as this would require negative terms in the sum.

The sum rules themselves do not tell us how rapidly they converge. The changes that we make on the lowest energy states are typically so drastic at the higher fields used in experiments that we may not evaluate them by low-order perturbation theory. Generally, however, higher energy states will be more difficult to perturb, and consequently, we should expect changes in absorption associated with them to become progressively smaller, leading to convergence of the absorption sum rules with finite energy range of integration.

One important factor implicit in all the sum rules is the existence of "forbidden" transitions. It is typical when perturbing the system with, for example, electric field to reduce the overlap and hence the strength of the allowed transitions. The way in which the sum rule continues to be obeyed is through the growth of forbidden transitions. A clear experimental example of the growth of these for-

bidden transitions is seen in the excitonic absorption spectra of cuprous oxide [47] where, with applied field, various new lines appear. This sum rule should apply to such spectra when taken over a sufficiently large energy range. Another interesting example is in the theoretical spectra for the quantum-confined Franz–Keldysh effect [35]. In this simplified case where excitonic effects are neglected, the growth of forbidden transitions between valence and conduction subbands is responsible for the transition from QCSE-like behavior to the Franz–Keldysh-like behavior.

### D. Comparison to Experiment

*1) Sum Rule 1:* This sum rule, which predicts overall conservation of integrated absorption, seems to agree very well with the observation noted in Section III-B5) that the area of the spectra in both polarizations is conserved over the photon range measured. Nevertheless, the experimental behavior for the light hole spectra [Fig. 2(b)] is still hard to understand because we are unable to explain the cause of the rise of absorption at high photon energies in these spectra. After the lowest energy, $n = 1$ electron to $n = 1$ lh transition, the next lh transition is the $n = 1$ electron to $n = 2$ lh transition which we calculate lies at an energy of 1.52–1.55 eV depending on field; this is too high to explain our result. The explanation may lie in a breakdown of the effective mass approximation away from the Brillouin zone center, and it is worth noting that the sum rule is valid even if we cannot evaluate the detailed energies and wavefunctions.

As mentioned above, this sum rule is more generally applicable to electroabsorption. We have reexamined the original data for *parallel field* electroabsorption in quantum wells [20]. This electroabsorption is qualitatively similar to that seen in low-temperature bulk semiconductors, primarily showing a broadening of the excitonic features. We find that over the spectral range measured (1.435–1.475 eV), the area is conserved within experimental error of ~5 percent for fields up to ~40 kV/cm. At higher fields, significant changes in the spectra are apparent at both ends of this range, implying that significant absorption changes occur with this range, and the conservation of area over this range starts to break down.

*2) Sum Rule 2:* This sum rule is applicable in the case of strong quantization, and predicts that the area of the absorption on a given "step" (i.e., a particular valence subband to conduction subband transition), including the excitonic effects of the Coulomb correlation of motion in the plane, is proportional to the square of the $z$ overlap, provided that we integrate over all the in-plane states that are significantly perturbed. We certainly expect that the lowest excitonic state will be significantly perturbed; its radius in the plane may increase by ~30 percent with field perpendicular to the layers [20], greatly reducing the lateral overlap of this state. The sum rule implies that other transitions, possibly "forbidden," will increase in strength to conserve overall area. For example, nominally $P$ excitons may become partly allowed. It is possible that the consequence of the reduction in strength of allowed transitions combined with the growth of the forbidden transitions will lead to a broadening of the excitonic resonance features when these transitions are not independently resolved; this is a possible explanation for the broadening of the exciton resonance being larger than predicted solely on the basis of lifetime effects discussed in Section III-B1).

Whether or not the growth of forbidden transitions is the explanation of the broadening, it is empirically clear that the area under the nominal exciton resonance is conserved [as discussed in Section III-B3)], which is in agreement with this sum rule. What is not clear is why this sum rule appears to converge so rapidly.

*3) Sum Rule 3:* This sum rule, which applies to the heights of the "steps" with excitonic effects neglected, states that the total height of all steps from a given subband is a constant (considering only one type of hole at a time). A particularly relevant application of this is to the transitions between the first electron subband and the heavy hole subbands. This can be seen very clearly, for example, in the calculated spectra for a 100 Å infinite well at 100 kV/cm [35]. The $n = 1$ hh to $n = 1$ electron transition loses strength with field, but this is almost entirely recovered by the growth of the $n = 2$ hh to $n = 1$ electron transition, with the remainder being made up by the $n = 3$ hh to $n = 1$ transition. The consequence of this is that before the $n = 2$ hh to $n = 2$ electron step, the original height of the $n = 1$ to $n = 1$ transition is totally recovered, i.e., the absorption on the plateau between the $n = 1$ and $n = 2$ hh to conduction allowed transition energies remains essentially constant with field. This can be clearly seen, for example, in the spectra in [18], and it is apparent on the hh spectra in Fig. 2(a) where the original step height is essentially recovered after the $n = 2$ hh to $n = 1$ electron transition, as discussed in Section III-B4) above.

## V. Conclusions

The experimental investigation of quantum well waveguides has shown particularly clear absorption spectra, with the light hole transitions clearly displayed when the optical electric vector is perpendicular to the layers. This configuration has enabled the demonstration of modulators and self electrooptic effect devices with polarization-dependent properties and with large modulation depths. Analysis of the spectra has yielded quantitative information on exciton broadening and absorption strengths without many of the inhomogeneous effects of previous measurements.

As a result of a body of work, the physics of absorption and luminescence near the bandgap of quantum wells in the presence of fields perpendicular to the layers can now be explained in a relatively consistent and complete way. The fields cause the absorption including the exciton peaks to shift through the quantum-confined Stark effect; the inhibition of field ionization allows the exciton to persist. The luminescence lifetime increases due to the loss of overlap between electron and hole as they are pulled to

the opposite sides of the well. If the well is too narrow or the barriers are too thin, the particle lifetime will decrease due to tunneling. The strength of the luminescence also decreases as the overlap is reduced. In this paper, we have been able to make a good quantitative comparison between theory and experiment for the associated changes in absorption strength in the presence of field. We have included the effect of excitons by deriving sum rules. Forbidden transitions are important for a full understanding of the absorption behavior, even when they are not resolved spectrally.

In conclusion, the electric field dependence of linear optical properties in quantum well has exposed some interesting new mechanisms not available in bulk semiconductors and has opened up several new devices possibilities. Further physics and applications will doubtless follow as the ability to fabricate ever more sophisticated sructures continues to advance.

## ACKNOWLEDGMENT

We would like to acknowledge the contributions of our colleagues C. A. Burrus, A. C. Gossard, J. E. Henry, W. Wiegmann, and T. H. Wood in making the experiments possible, and stimulating discussions on sum rules with S. Schmitt-Rink.

## REFERENCES

[1] R. Dingle, "Confined carrier quantum states in ultrathin semiconductor heterostructures," *Festkorperprobleme (Advances in Solid State Physics), Vol XV*, H. J. Queisser, Ed. Braunschweig: Pergamon/Vieweg, 1975, pp. 21-48.

[2] D. S. Chemla and D. A. B. Miller, "Room-temperature excitonic nonlinear-optical effects in semiconductor quantum-well structures," *J. Opt. Soc. Amer.*, vol. B2, pp. 1155-1173, 1985.

[3] E. E. Mendez, G. Bastard, L. L. Chang, L. Esaki, H. Morkoc, and R. Fischer, "Effect of an electric field on the luminescence of GaAs quantum wells," *Phys. Rev.*, vol. B26, pp. 7101-7104, 1982.

[4] M. Yamanishi and I. Suemune, "Quantum mechanical size effect modulation light sources—A new field effect semiconductor laser or light emitting device," *Japan. J. Appl. Phys.*, vol. 22, pp. L22-L24, 1983.

[5] G. Bastard, E. E. Mendez, L. L. Chang, and L. Esaki, "Variational calculations on a quantum well in an electric field," *Phys. Rev.*, vol. B28, pp. 3241-3245, 1983.

[6] D. S. Chemla, T. C. Damen, D. A. B. Miller, A. C. Gossard, and W. Wiegmann, "Electroabsorption by Stark effect on room-temperature excitons in GaAs/GaAlAs multiple quantum well structures," *Appl. Phys. Lett.*, vol. 42, pp. 864-866, 1983.

[7] R. C. Miller and A. C. Gossard, "Some effects of a longitudinal electric field on the photoluminescence of p-doped $GaAsAl_xGa_{1-x}As$ quantum well heterostructures," *Appl. Phys. Lett.*, vol. 43, pp. 954-956, 1983.

[8] T. H. Wood, C. A. Burrus, D. A. B. Miller, D. S. Chemla, T. C. Damen, A. C. Gossard, and W. Wiegmann, "High-speed optical modulation with GaAs/GaAlAs quantum wells in a p-i-n diode structure," *Appl. Phys. Lett.*, vol. 44, pp. 16-18, 1984.

[9] D. A. B. Miller, D. S. Chemla, T. C. Damen, A. C. Gossard, W. Wiegmann, T. H. Wood, and C. A. Burrus, "Novel hybrid optically bistable switch: The quantum well self-electro-optic effect device," *Appl. Phys. Lett.*, vol. 45, pp. 13-15, 1984.

[10] —, "Band-edge electroabsorption in quantum well structures: The quantum-confined Stark effect," *Phys. Rev. Lett.*, vol. 53, pp. 2173-2176, 1984.

[11] J. A. Brum and G. Bastard, "Electric-field-induced dissociation of excitons in semiconductor quantum wells," *Phys. Rev.*, vol. B31, pp. 3893-3898, 1985.

[12] T. H. Wood, C. A. Burrus, D. A. B. Miller, D. S. Chemla, T. C. Damen, A. C. Gossard, and W. Wiegmann, "131 ps optical modulation in semiconductor multiple quantum wells (MQW's)," *IEEE J. Quantum Electron.*, vol. QE-21, pp. 117-118, 1985.

[13] C. Alibert, S. Gaillard, J. A. Brum, G. Bastard, P. Frijlink, and M. Erman, "Measurements of electric-field induced energy-level shifts in GaAs single-quantum-wells using electroreflectance," *Solid State Commun.*, vol. 53, pp. 457-460, 1985.

[14] D. A. B. Miller, D. S. Chemla, T. C. Damen, T. H. Wood, C. A. Burrus, A. C. Gossard, and W. Wiegmann, "Optical-level shifter and self-linearized optical modulator using a quantum-well self-electro-optic effect device," *Opt. Lett.*, vol. 9, pp. 567-569, 1984.

[15] M. Yamanishi, Y. Kan, T. Miname, I. Suemune, H. Yamamoto, and Y. Usami, "Quenching of photoluminescence from GaAs/AlGaAs single quantum well by an electric field at high temperature," *Superlattices and Microstruct.*, vol. 1, pp. 111-113, 1985.

[16] M. Yamanishi, H. Yamamoto, and I. Suemune, "Size effect modulation light sources—Possibility of LED mode operation at room temperature," *Superlattices and Microstruct.*, vol. 1, pp. 335-337, 1985.

[17] J. A. Kash, E. E. Mendez, and H. Morkoc, "Electric field induced decrease of photoluminescence lifetime in GaAs quantum wells," *Appl. Phys. Lett.*, vol. 46, pp. 173-175, 1985.

[18] H. Iwamura, T. Saku, and H. Okamoto, "Optical absorption of GaAs-AlGaAs superlattice under electric field," *Japan. J. Appl. Phys.*, vol. 24, pp. 104-105, 1985.

[19] D. A. B. Miller, D. S. Chemla, T. C. Damen, T. H. Wood, C. A. Burrus, A. C. Gossard, and W. Wiegmann, "The quantum well self-electro-optic effect device: optoelectronic bistability and oscillation, and self-linearized modulation," *IEEE J. Quantum Electron.*, vol. QE-21, pp. 1462-1476, 1985.

[20] D. A. B. Miller, D. S. Chemla, T. C. Damen, A. C. Gossard, W. Wiegmann, T. H. Wood, and C. A. Burrus, "Electric field dependence of optical absorption near the band gap of quantum-well structures," *Phys. Rev.*, vol. B32, pp. 1043-1060, 1985.

[21] E. J. Austin and M. Jaros, "Electronic structure of an isolated GaAs-GaAlAs quantum well in a strong electric field," *Phys. Rev.*, vol. B31, pp. 5569-5572, 1985.

[22] K. Wakita, Y. Kawamura, Y. Yoshikuni, and H. Asahi, "Electroabsorption on room-temperature excitons in InGaAs/InGaAlAs multiple quantum-well structures," *Electron. Lett.*, vol. 21, pp. 338-340, 1985.

[23] E. J. Austin and M. Jaros, "Electric field induced shifts and lifetimes in GaAs-GaAlAs quantum wells," *Appl. Phys. Lett.*, vol. 47, pp. 274-276, 1985.

[24] S. Tarucha, H. Iwamura, T. Saku, and H. Okamoto, "Waveguide-type optical modulator of GaAs quantum well double heterostructures using electric field effect on exciton absorption," *Japan. J. Appl. Phys.*, vol. 24, pp. L442-L444, 1985.

[25] T. H. Wood, C. A. Burrus, A. H. Gnauck, J. M. Wiesenfeld, D. A. B. Miller, D. S. Chemla, and T. C. Damen, "Wavelength-selective voltage-tunable photodetector made from multiple quantum wells," *Appl. Phys. Lett.*, vol. 47, pp. 190-192, 1985.

[26] K. Wakita, Y. Kawamura, Y. Yoshikuni, and H. Asahi, "High-temperature excitons and enhanced electroabsorption in InGaAs/InAlAs multiple quantum wells," *Electron. Lett.*, vol. 21, pp. 574-576, 1985.

[27] H. Yamamoto, M. Asada, and Y. Suematsu, "Electric-field-induced refractive index variation in quantum-well structure," *Electron. Lett.*, vol. 21, pp. 579-580, 1985.

[28] T. H. Wood, C. A. Burrus, R. S. Tucker, J. S. Weiner, D. A. B. Miller, D. S. Chemla, T. C. Damen, A. C. Gossard, and W. Wiegmann, "100 ps waveguide multiple quantum well (MQW) optical modulator with 10:1 on/off ratio," *Electron. Lett.*, vol. 21, pp. 693-694, 1985.

[29] J. S. Weiner, D. A. B. Miller, D. S. Chemla, T. C. Damen, C. A. Burrus, T. H. Wood, A. C. Gossard, and W. Wiegmann, "Strong polarization-sensitive electroabsorption in GaAs/AlGaAs quantum well waveguides," *Appl. Phys. Lett.*, vol. 47, pp. 1148-1150, 1985.

[30] S. Tarucha and H. Okamoto, "Monolithic integration of a laser diode and an optical waveguide modulator having a GaAs/AlGaAs quantum well double heterostructure," *Appl. Phys. Lett.*, vol. 48, pp. 1-3, 1986.

[31] H.-J. Polland, L. Schultheis, J. Kuhl, E. O. Gobel, and C. W. Tu, "Lifetime enhancement of two-dimensional excitons by the quantum-confined Stark effect," *Phys. Rev. Lett.*, vol. 55, pp. 2610-2613, 1985.

[32] R. T. Collins, K. von Klitzing, and K. Ploog, "Photocurrent spectroscopy of $GaAs/Al_xGa_{1-x}As$ quantum wells in an electric field," postdeadline paper presented at the Conf. Electron. Properties of Two-Dimensional Syst. (EP2DS VI), Kyoto, Japan, Sept. 1985.

[33] T. Miyazawa, S. Tarucha, Y. Ohmori, and H. Okamoto, "Room temperature observation of exciton and its electric field effect in GaSb-$Al_xGa_{1-x}Sb$ multi quantum wells," postdeadline paper P1 presented at the 2nd Int. Conf. Modulated Semiconductor Struct., Kyoto, Japan, Sept. 1985.
[34] K. Yamanaka, T. Fukunaga, N. Tsukada, K. L. I. Kobayashi, and M. Ishii, "Photocurrent spectroscopic observation of interband transition in GaAs-AlGaAs quantum wells under an applied high electric field," paper 18S presented at the 2nd Int. Conf. Modulated Semiconductor Struct., Kyoto, Japan, Sept. 1985.
[35] D. A. B. Miller, D. S. Chemla, and S. Schmitt-Rink, "The relation between electroabsorption in bulk semiconductors and in quantum wells: The quantum-confined Franz-Keldysh effect," *Phys. Rev. B*, to be published.
[36] W. H. Knox, D. A. B. Miller, T. C. Damen, D. S. Chemla, C. V. Shank, and A. C. Gossard, "Subpicosecond excitonic electroabsorption in room-temperature quantum wells," *Appl. Phys. Lett.*, vol. 48, pp. 864–866, 1986.
[37] C. Trallero Giner and J. Lopez Gondar, "Exact wave functions and energy levels for a quantum well with an applied electric field," *Physica B & C*, to be published.
[38] S. Schmitt-Rink, D. S. Chemla, and D. A. B. Miller, "Theory of transient excitonic optical nonlinearities in semiconductor quantum-well structures," *Phys. Rev.*, vol. B32, pp. 6601–6609, 1985.
[39] P. W. Smith, Y. Silberberg, and D. A. B. Miller, "Mode locking of semiconductor diode lasers using saturable excitonic nonlinearities," *J. Opt. Soc. Amer.*, vol. B2, pp. 1228–1236, 1985.
[40] In [21] and [23], only the tunneling broadening of hole states is presented, on the reasoning that the dominant shift is due to holes. However, for a given potential barrier, the electron (and the light hole) tunnel much more easily than does the heavy hole because of their lighter mass. With the currently fashionable ~60:40 split of the band discontinuities between conduction and valence bands, the electron tunneling is generally much stronger than the heavy hole tunneling as is shown explicitly in the calculations in [20], and hence should contribute a greater broadening even though thee may be relatively little shift of the electron state. This would help explain the discrepancy between the experiment [17] and the theoretical lifetimes [23].
[41] T. Lukes, G. A. Ringwood, and B. Suprapto, "A particle in a box in the presence of an electric field and applications to disordered systems," *Physica*, vol. 84A, pp. 421–434, 1976.
[42] F. M. Fernandez and E. A. Castro, "Hypervirial-perturbational treatment of a particle in a box in the presence of an electric field," *Physica*, vol. 111A, pp. 334–342, 1982.
[43] J. S. Weiner, D. S. Chemla, D. A. B. Miller, H. A. Haus, A. C. Gossard, W. Wiegmann, and C. A. Burrus, "Highly anisotropic optical properties of single quantum well waveguides," *Appl. Phys. Lett.*, vol. 47, pp. 664–667, 1985.
[44] H. A. Haus and D. A. B. Miller, "Attenuation of cutoff modes and leaky modes of dielectric slab structures," *IEEE J. Quantum Electron.*, vol. QE-22, pp. 310–324, 1986.
[45] D. S. Chemla, D. A. B. Miller, P. W. Smith, A. C. Gossard, and W. Wiegmann, "Room temperature excitonic nonlinear absorption and refraction in GaAs/AlGaAs multiple quantum well structures," *IEEE J. Quantum Electron.*, vol. QE-20, pp. 265–275, 1984.
[46] O. Madelung, *Introduction to Solid-State Theory*. New York: Springer-Verlag, 1978.
[47] M. Grosmann, "The effect of perturbations upon the excitonic spectrum of cuprous oxide," in *Polarons and Excitons*, C. G. Kuper and G. D. Whitfield, Eds. London: Oliver & Boyd, 1963, pp. 373–381.

**David A. B. Miller**, for a photograph and biography, see p. 318 of the February 1986 issue of this JOURNAL.

**Joseph S. Weiner** was born in Providence, RI, on June 9, 1955. He received the A.B. degree in physics from Princeton University, Princeton, NJ, in 1977 and the M.A. and Ph.D. degrees in physics from the University of California, Berkeley. His thesis work was on time-resolved luminescence and resonant Raman scattering in semiconductors.

From 1984 to 1986 he was a Post Doctoral Fellow at AT&T Bell Laboratories, Holmdel, NJ, in the Quantum Physics and Electronics Research Department. He is currently a member of the Technical Staff in the Solid State Electronics Research Laboratory, AT&T Bell Laboratories, Murray Hill, NJ. His research interests include the physics of quantum wells and microstructures.

**D. S. Chemla**, for a photograph and biography, see this issue, p. 1610.